Determining thermal noise limiting properties of thin films

Courtney Linn
Institute for Gravitational Research
University of Glasgow
Summer 2011

Abstract

In order to make thermally stable mirrors to be used for LIGO interferometers, the thermal properties for thin layer materials must be measured, specifically the elastic modulus and mechanical loss. In the nano-indentation experiment, a diamond tip indenter is pressed onto a sample at specific loads, varying from 100 N to 10,000 N. The indenter records the depth the indenter travels for every force placed on the sample, and from this data, multiple material properties can be extracted, with the elastic modulus being the most relevant material property to this experiment. In a separate experiment, the elastic modulus was determined for ion-beam sputtered cantilevers by viewing the change in the radius of curvature as a function of temperature. From these experiments, the elastic modulus of Ta_2O_5 deposited on SiO_2 was found as determined by the thermal bending experiment, and the elastic modulus was found for Ta_2O_5, and elastic moduli for various heat treating temperature and doping at $25 - 55\%$ with TiO_2. In the mechanical loss experiment, a the loss for an uncoated reference sample of silicon and a coated silicon cantilever with an amorphous silicon coating were measured using a cryostat.

1 Introduction

The motivation for this project is for use in creating higher sensitivity instruments in the search for gravitational waves. Determining the elastic modulus of thin films for use in interferometric detectors allows scientist to select materials with less internal friction, which greatly reduces the overall noise in the detector.

2 Mechanical Loss Experiment

2.1 Background and Theory

The mechanical loss of a material is a measure of the loss of energy due to internal friction in the material. This is measurable by placing a cantilever in a cryostat as shown in the diagram above. The cantilever is excited to its specific vibrational modes, and then the energy dampens and the ringdown is recorded. To find the frequency of the nth bending mode of a cantilever,

$$\omega_n = (k_n L)^2 \frac{a}{2\sqrt{3}L^2}\sqrt{\frac{Y}{\rho}} \tag{1}$$

where n is mode number, Y is elastic modulus, ρ is density, a is thickness of the cantilever, L is the length of the cantilever, and $(k_n L)^2$ is given by:

$$k_n L = \frac{(2n-1)\pi}{2}$$

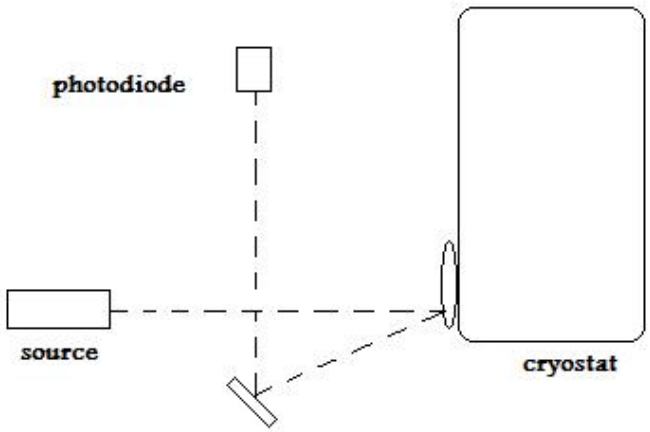

Figure 1: The above is a schematic of the setup used to detect the motion of the cantilever. The laser is reflected off of the vibrating cantilever and the beam is directed onto a pair of photodiodes. Changes in the beam position on the photodiodes are due to the vibration of the cantilever.

In the cryostat, non-internal friction sources of energy loss are removed by creating a vacuum to eliminate the cantilever's collision with air molecules, and the chamber encasing the cantilever is cooled to eliminate energy loss from thermal excitations. Thermoelastic loss, a source of energy loss caused by the oscillating compression and tension of the vibrating cantilever that causes an oscillating heat flow, is accounted for by the follwing equation:

$$\phi(\omega) = \frac{Y\alpha^2 T}{\rho C}\frac{\omega\tau}{1+\omega^2\tau^2} \tag{2}$$

where T is temperature, C is specific heat capacity, ω is frequency, τ is the relaxation time, and the following expression for relaxation time of a cantilever:

$$\tau = \frac{\rho C t^2}{\pi^2 \kappa} \tag{3}$$

where t is the thickness of the cantilever and κ is the thermal conductivity.

Physically, the relaxation time is an effect caused by a time delay in the strain response from a stress applied to an anelastic material. For an oscillating stress

$$\sigma = \sigma_0 e^{i2\pi f t},$$

strain has a linear relationship and is periodic with the same angular frequency but with a phase lag ϕ with respect to stress, where:

$$\phi(f_0) = \frac{E_{\text{lost per cycle}}}{2\pi E_{\text{stored}}} \tag{4}$$

2.2 Experiment and Procedures

The samples used were reference sample 5, an uncoated Si cantilever, and sample 2, a cantilever with a Si substrate with an amorphous Si coating. During the data runs, the Lakeshore Temperature Controller changed the temperature from 8-300K, exciting the cantilever to 5 vibrational modes, and the LabVIEW program recorded the ringdown of energy loss in the cantilever as a function of time. The following plots show a sample frequency scan and a corresponding ringdown. The peak for the frequency scan represents the vibrational mode the cantilever reached,

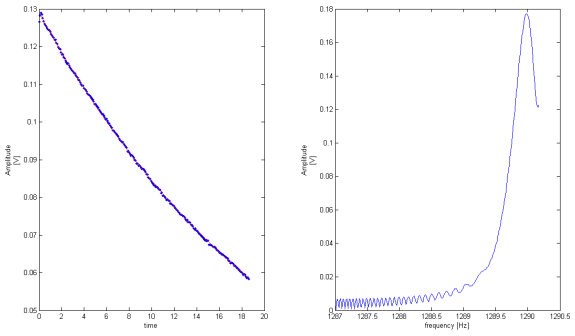

Figure 2:

and the exponential fit to the ringdown gives a calculation for the mechanical loss.

2.3 Data and Analysis

The following plots show how the calculated loss changed as a function of temperature for both uncoated silicon and amorphous silicon on silicon.

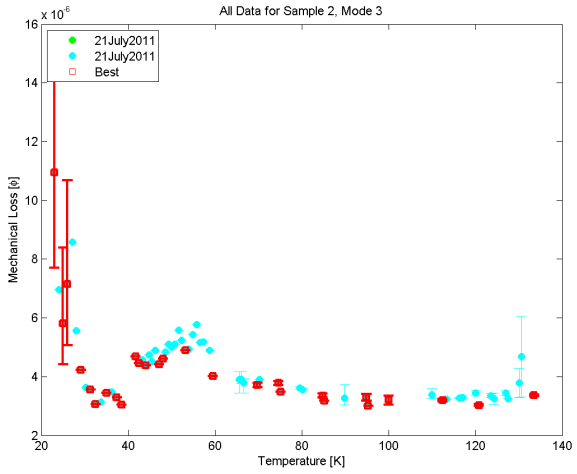

Figure 3: The above is a plot of ϕ versus T (temperature) for the amorphous silicon coated cantilever.

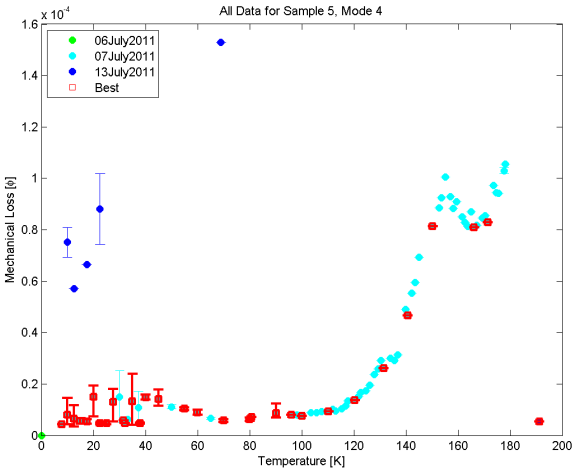

Figure 4: The above is a plot of ϕ versus T (temperature) for the uncoated silicon reference cantilever.

Because acquiring mechanical loss data is time consuming, not enough quality data was collected, and an upper limit for amorphous silicon was determined to be around $5x10^{-6}$. To determine the loss of the amorphous silicon coating, the loss of the uncoated reference sample is subtracted from the loss of the coated sample. The loss of the amorphous silicon coating did not contribute enough to the loss of the coated sample to extract a viable number, especially considering the too few quality data sets. To test this further, more data should be taken, and having amorphous silicon on a substrate with a lower loss than silicon should be considered.

3 Thermal Bending Experiment

3.1 Background and Theory

In the thermal bending experiment, an ion-beam sputtered cantilever with a substrate made of SiO_2 is spherically curved due to the coating procces, during which Ta_2O_5 was placed onto the substrate. By uniformly heating the cantilever in an insulated box and measuring the radius of curvature of the cantilever at room temperature and at every incremental increase in temperature, the elastic modulus can be calculated.
From the diagram above, x is the distance between the two beams exiting the beam splitter/mirror, L is the total length travelled by reflected beams, δ is the separation of reflected beams, measured on a wall. From geometric optics,

$$f = \frac{R}{2} \tag{5}$$

where f is the focal length of the cantilever. From the above diagram,

$$R = \frac{2Lx}{\delta} \tag{6}$$

where R is the radius of curvature of the cantilever. From Stoney's

$$\sigma = \frac{B_s t_s^2}{6 t_f R} = (\alpha_s - \alpha_f) B_f T \tag{7}$$

wnere t_s is the thickness of the substrate, t_f is the thickness of the film, and B_s is the biaxial modulus of the substrate, given by:

$$B = \frac{E}{1 - v} \tag{8}$$

where v is the Poisson's ratio of the material, a ratio of the contraction (perpendicular to the load) and extention (parallel to load) that occurs when a material is stretched, which is assumed to be 0.2.
By solving for B_f from the two expressions in Eq. (3),

$$B_f = \frac{d\delta}{dT} \frac{B_s t_s^2}{12 L x \delta \alpha t_f} \tag{9}$$

3.2 Experiment and Procedures

The apparatus must be set up as the diagram previously shown and the experimentalist must ensure that the beams exiting the beam splitter and reflecting off the mirror are completely parallel. This can be achieved by placing a flat mirror in front of the sample box and ensuring that the distance between the beams is the same along the beam's path. For a data set, the temperature inside the box from the Lakeshore 340 Temperature Controller (T), the distance between the beams exiting the beam splitter and being reflected off of the mirror (x), the distance from the beam's reflection point off of the cantilever to the point on the opposing wall

where the beams appear (L), and the distance between reflected beams on the wall (δ) all must be measured and recorded for every steady level of temperature reached. In general, a waiting period of 90 minutes was given between changes in temperature to ensure a steady state had been reached.

3.3 Data and Analysis

The following is a plot of $\frac{1}{R}$ versus T (temperature) for each position of the laser beams x.

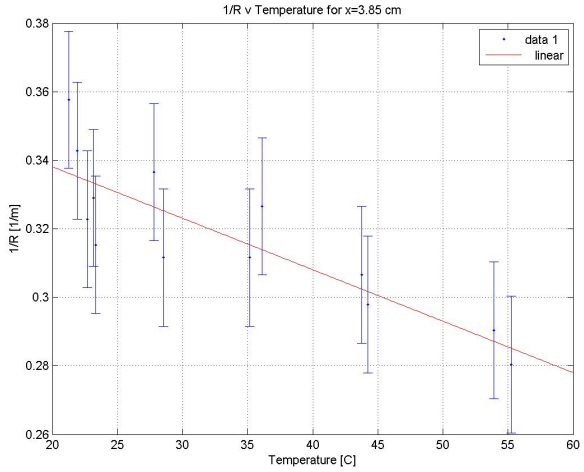

Figure 5: The above is a plot of $\frac{1}{R}$ versus T (temperature) for the position of the beams where $x = 3.85$ cm.

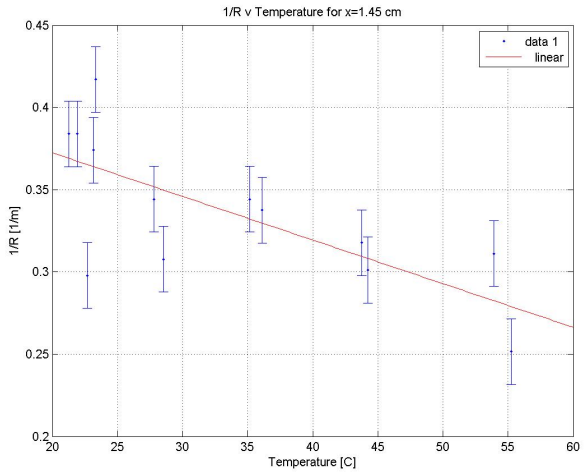

Figure 6: The above is a plot of $\frac{1}{R}$ versus T (temperature) for the position of the beams where $x = 1.45$ cm.

From these plots, a composite elastic modulus and linear expansion coefficient was determined. Using the elastic modulus for Ta_2O_5 from the nanoindentation data, the linear expansion coefficient was found to be $3.43x10^{-6}\frac{1}{^\circ C}$.

To calculate the error in the calculation of radius of curvature, 4 identical mirrors' focal lengths were measured using the laser configuration from the thermal bending setup as well as with a spherometer. The measurements from the spherometer and the thermal bending setup were at most 2 cm in error with an average of 62.2 cm for focal length.

4 Nanoindentation Experiment

4.1 Experiment and Procedures

The data collection for the nano-indentation experiment was done at Cambridge University using their indenter with a Berkovich tip. During nano-indentation testing, the depth an indenter travels is recorded as well as the load placed on the indenter to deform a sample. With the Cambridge indenter, we performed 25 indents in 3 locations per sample, with each indent within the location 10 microns apart. The following schematic is a representation of the deformation the indenter causes to the sample.

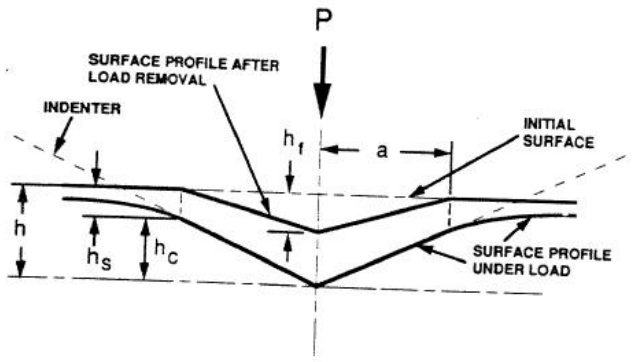

Figure 7: The above is a schematic of an indenter and the impressions in makes on a film-substrate system.

4.2 Data and Analysis

In nanoindentation, an indenter is pressed against a material and the load P and depth the indenter travels h during the loading and unloading are recorded, and the elastic modulus is determined from

$$E^* = \frac{\sqrt{\pi}}{2}\frac{dP}{dh}\frac{1}{\sqrt{A}} \tag{10}$$

where E^* is the sample and indenter combined modulus, A is the projected area of contact of the indenter under load, and $\frac{dP}{dh}$ is the slope of the load-depth curve for plastic and elastic deformation of the sample. The sample modulus E is then determined using:

$$\frac{1}{E^*} = \frac{1}{E'} + \frac{1}{E'_{\text{indenter}}} \tag{11}$$

where

$$E' = \frac{E}{1-v^2}$$

and E' is the reduced modulus of the sample, E is the elastic modulus of the sample, and v is Poisson's ratio.

The reduced moduli is used because it represents the mean value of the elastic modulus in the indented zone, taking into account the inhomogeneous contact stresses and strains. E and $E^{'}$ are both composite moduli of both the film and substrate. Because in most causes of samples the film modulus E_f differs from the substrate modulus E_s, the measured $E^{'}$ changes as a function of depth h such that:

$$E^{'} = E_s + (E_f - E_s)\Phi(x)$$

or

$$E^{'} = E_f + (E_s - E_f)\Psi(x)$$

where Φ is a function of relative penetration depth x and Φ=1 for no penetration and Φ tends to 0 for large depths. Then:

$$\Psi = 1 - \Phi$$

Letting $\Phi(x) = e^{-\alpha x}$, where α is a constant and x is depth the indenter has traveled, finding both the elastic modulus of the substrate and film as a function of depth is possible. The following fit is a representation of the described model for finding the elastic modulus of the film and substrate.

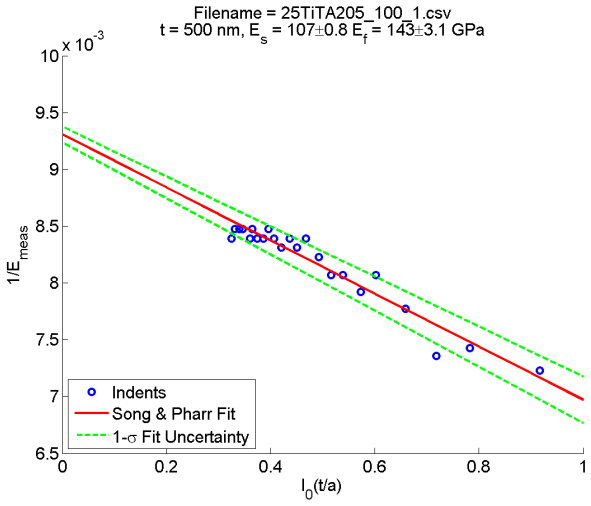

Figure 8: The above graph shows indents as circles and shows the fit and error in the fit to the Φ function.

5 Acknowledgements

I'd like to give a special thanks to the University of Florida and the National Science Foundation for supporting and organizing this summer's research experience. I couldn't have done any of this without the help, wisdom, and patience of Dr. Iain Martin and Matt Abernathy.

6 References

Saulson, Peter R. Fundamentals of Interferometric Gravitational Wave Detectors. World Scientific Publishing,(1994).
C. Zener, Internal friction in solids I. Theory of internal friction in reeds, Physical Review, 52, (1937) 230-235.
A. Nowick, B. Berry, Anelastic Relaxation In Crystalline Solids, Academic Press, NY, 1972.
J. Mencik, D. Munz, Determination of elastic modulus of thin layers using nanoindentation, Journal of Materials Research, 12, (1997) 2475-2484.
J. Mencik, Elastic modulus of TbDyFe films-a comparison of nanoindentation and bending measurements, Thin Solid Films, 287, (1996) 208-213.
W.C. Oliver, G.M. Pharr, An inproved technique for determining hardness and elastic modulus using load and displacement sensing indentation experiments. J. Mater. Res., 7, (1992) 1564-1583.
V.B. Braginsky, A.A. Samoilenko, Measurements of the optical mirror coating properties, Physics Letters A, 315, (2003) 175-177.